

# JEDI: Adaptive Stochastic Estimation for Joint Enhancement and Despeckling of Images for SAR

Wen Zhang  
wen.zhang@ieee.org

Alexander Wong  
alexanderwong@ieee.org

David A. Clausi  
dclausi@uwaterloo.ca

Vision and Image Processing Group  
Systems Design Engineering  
University of Waterloo  
Waterloo, Ontario, Canada N2L 3G1

## Abstract

*Synthetic aperture radar (SAR) images are degraded by a form of multiplicative noise known as speckle. Current methods for despeckling are limited in that they either do not perform enough noise attenuation, or do not adequately preserve or enhance image detail. We propose a novel adaptive stochastic method for joint enhancement and despeckling of images (JEDI) for SAR. The proposed method utilizes an adaptive importance sampling scheme based on local statistics to generate random samples while reducing estimation variance. A Monte Carlo estimate is computed based on the generated samples, wherein the samples are aggregated to form a despeckled and detail-enhanced result. The advantage of JEDI is the ability to efficiently take advantage of information redundancy in speckled images to reduce the effects of speckle while simultaneously enhancing detail visualization. Testing with both simulated and real speckled images shows that JEDI typically outperforms popular despeckling algorithms such as Frost filtering, anisotropic diffusion, median filtering,  $\Gamma$ -MAP and GenLik in terms of quantitative and qualitative visual quality. On average, JEDI provides a 2-15% improvement in PSNR and a 5-14% improvement in image quality index measures over the tested methods.*

## 1 Introduction

Synthetic aperture radar (SAR) is a widely-used technology in remote sensing applications. SAR images are generated by measuring the backscattered signal from a radio pulse. Because of phase coherence effects caused by multiple scatterers in a resolution cell, the resulting images are characterized by a grainy pattern known as speckle [1]. Popular speckle reduction methods include linear least-

squares estimators (LLSE) based on local statistics, such as the Lee [2], Frost [3], and Kuan [4] filters. Other despeckling methods include  $\Gamma$ -MAP [5], anisotropic diffusion [6], adaptive weighted median filtering [7], and wavelet-domain filtering (GenLik) [8].

A limitation of current despeckling methods is insufficient noise attenuation in homogeneous regions, especially with correlated speckle. Moreover, while current despeckling methods are designed to preserve edges, they do not enhance them for better visibility, and often do not provide speckle reduction in edge regions. These problems can limit the visual quality of the despeckled image, as well as create difficulties for automatic segmentation techniques, to such an extent that SAR smoothing is not performed in these approaches [9].

The current methods all depend, to varying extents, on local information redundancy. Recently, Wong et al. [10] proposed a Monte Carlo estimation framework for denoising that allows efficient use of global information redundancy. Based on this, we propose a novel method for joint enhancement and despeckling of images (JEDI) that employs an adaptive stochastic approach to overcome limitations inherent in local methods. The proposed JEDI method is able to attain greater levels of speckle attenuation while increasing the visibility of image structures.

## 2 Adaptive Stochastic Estimation

### 2.1 Speckle Model

Let  $S$  be the discrete lattice on which the images  $f$ ,  $g$ , and random field  $n$  are defined, and let  $\mathbf{x}$  be an index into the lattice. Speckle, which arises from the constructive and destructive interference of the backscattered signal, can be modeled as multiplicative noise [1] according to

$$g(\mathbf{x}) = f(\mathbf{x}) \cdot n(\mathbf{x}), \quad (1)$$

where  $g(\mathbf{x})$  is the observed signal intensity at lattice location  $\mathbf{x} = [x \ y]^T$ ,  $f(\mathbf{x})$  is the “noise-free” signal, and  $n(\mathbf{x})$  is the fading variable. The fading variable can be modeled as a stationary random process with  $E[n(\mathbf{x})] = 1$  that is assumed to be independent of the noise-free signal  $f(\mathbf{x})$ . For fully developed speckle, it can be shown that the measured backscatter amplitude follows a Rayleigh distribution [1], and has a probability density function (pdf) given by

$$p(g|\sigma_g) = \frac{g}{\sigma_g^2} \exp\left(-\frac{g^2}{2\sigma_g^2}\right) \quad (2)$$

$$g \in [0, \infty),$$

where  $\sigma_g$  is the shape parameter which depends on the reflectance of the scatters in the resolution cell.

## 2.2 Estimation Framework

Since the noise-free signal  $f(\mathbf{x})$  and the fading variable  $n(\mathbf{x})$  are assumed to be independent, the expected value of the observed image signal  $g(\mathbf{x})$  becomes

$$\begin{aligned} E[g(\mathbf{x})] &= E[f(\mathbf{x}) \cdot n(\mathbf{x})] \\ &= E[f(\mathbf{x})] \cdot E[n(\mathbf{x})] \\ &= E[f(\mathbf{x})]. \end{aligned} \quad (3)$$

This implies that an estimate of the noise-free image signal  $f(\mathbf{x})$  can be obtained by taking the average of repeated measurements. However, it is not practical to image a region repeatedly over a small time-frame using SAR platforms. An alternative approach is to use a spatial domain estimation approach to make use of the information redundancy contained in the image itself. This type of estimate can be written in the form of a weighted sum

$$\hat{f}(\mathbf{x}) = \frac{1}{W(\mathbf{x})} \sum_{\xi \in \Omega_{\mathbf{x}}} w(\mathbf{x}, \xi) g(\xi), \quad (4)$$

where  $W(\mathbf{x})$  is the normalizing factor given by

$$W(\mathbf{x}) = \sum_{\xi \in \Omega_{\mathbf{x}}} w(\mathbf{x}, \xi), \quad (5)$$

and  $\Omega_{\mathbf{x}}$  is a set of indices into  $S$ . Methods that fall under this framework include the aforementioned Lee, Frost, and Kuan filters, where the weights are adaptively determined based on the local image statistics. If the weights  $w(\mathbf{x}, \xi)$  are identical and spatially-invariant, then we have a simple spatial average filter, which is the basis for multi-look despeckling. In the existing despeckling methods, the range of the summation is restricted such that  $\Omega_{\mathbf{x}}$  is a rectangular neighborhood centered at  $\mathbf{x}$ . One limitation to this restriction in summation range is that local information redundancy is often inadequate for reducing speckle in observed

image signals characterized by low signal-to-noise ratios. One effective approach to improving despeckling performance is to extend the summation such that  $\Omega_{\mathbf{x}} = S$ , thus fully exploiting information redundancy within the image. However, to estimate  $f(\mathbf{x})$  deterministically when  $\Omega_{\mathbf{x}} = S$  is not computationally feasible.

## 2.3 Joint Despeckling and Enhancement

Wong et al [10] showed that an efficient and effective way to improve the filtering given in Eq. 4 when  $\Omega_{\mathbf{x}} = S$  is to use a stochastic estimation approach. The goal is to take better advantage of the information redundancy contained in the image, while still being computationally efficient to compute.

Let  $p$  be a pdf on  $S$ , and  $\mathbf{x}_c$  be the pixel being estimated. Instead of using all image samples  $\xi \in S$ , we draw  $m$  random samples,  $\xi_1, \dots, \xi_m$ , using a pdf  $p(\xi|\mathbf{x}_c)$ . Hence, we have the Monte Carlo estimate of the pixel given by

$$\tilde{f}(\mathbf{x}_c) = \frac{1}{W(\mathbf{x}_c)} \sum_{i=1}^m w(\mathbf{x}_c, \xi_i) g(\xi_i) \quad (6)$$

$$W(\mathbf{x}_c) = \sum_{i=1}^m w(\mathbf{x}_c, \xi_i). \quad (7)$$

Given a large enough sample size, the Monte Carlo estimate  $\tilde{f}(\mathbf{x})$  approaches the deterministic estimate  $\hat{f}(\mathbf{x})$ . The main advantage of the proposed Monte Carlo filtering method is that it is significantly more computationally efficient than the deterministic spatial domain filtering approach when  $\Omega_{\mathbf{x}} = S$ , since a relatively small number of samples is necessary to achieve high despeckling performance.

We calculate the weights based on the similarity of the neighborhoods around  $\mathbf{x}_c$  and  $\xi_i$  according to

$$w(\mathbf{x}_c, \xi_i) = e^{-\frac{\Phi(\mathbf{x}_c, \xi_i)}{h^2}} \quad (8)$$

where  $h$  is a decay factor and  $\Phi(\mathbf{x}_c, \xi_i)$  represents the summed difference of the pixel neighbourhood intensities weighted by a Gaussian kernel  $G(\cdot)$

$$\Phi(\mathbf{x}_c, \xi_i) = \sum_{\delta} G(\delta) \cdot (g(\mathbf{x}_c - \delta) - g(\xi_i - \delta))^2. \quad (9)$$

To reduce estimation variance, the biasing density  $p$  used to compute the Monte Carlo estimate is adaptively chosen based on the proximity and perceptual similarity between the target pixel and the rest of the pixels within the image, such that

$$p(\xi|\mathbf{x}_c) = \frac{1}{C(\xi, \mathbf{x}_c)} e^{-\alpha|\mathbf{x}_c - \xi|^2 (\sigma^2(\xi) - \sigma^2(\mathbf{x}_c))^2}, \quad (10)$$

where  $\sigma^2(\cdot)$  is the local image variance and  $|\cdot|$  denotes the Euclidean distance between two pixel coordinates.  $C(\xi, \mathbf{x}_c)$

is a normalizing factor given by

$$C(\xi, \mathbf{x}_c) = \sum_{\xi} e^{-\alpha|\mathbf{x}_c - \xi|^2(\sigma^2(\xi) - \sigma^2(\mathbf{x}_c))^2}. \quad (11)$$

The constant  $\alpha$  controls the decay rate of the density function.

One of the underlying goals of JEDI is to improve image detail while reducing speckle for easier visual detection of features within an ultrasound image. To achieve joint despeckling and detail enhancement, we incorporate a stochastic detail emphasis term into the adaptive Monte Carlo estimation framework, according to

$$\begin{aligned} \hat{f}_{enh}(\mathbf{x}_c) &= \frac{\theta}{W_1(\mathbf{x}_c)} \sum_{i=1}^m e^{-\frac{\Phi(\mathbf{x}_c, \xi_i)}{h^2}} g(\xi_i) \\ &\quad - \frac{\theta - 1}{W_2(\mathbf{x}_c)} \sum_{i=1}^m e^{-\frac{\Phi(\mathbf{x}_c, \xi_i)}{\beta^2 n^2}} g(\xi_i), \end{aligned} \quad (12)$$

where the second term corresponds to a Monte Carlo estimate obtained by using a decay factor of  $\beta h$ . What this effectively does is adaptively amplify stochastically estimated image detail based on the difference of Monte Carlo estimates, with the level of enhancement controlled by the ratio factor  $\theta$ . In this case, the integration of detail enhancement into the adaptive Monte Carlo estimation framework comes at little extra cost since it is computed as part of same stochastic estimation procedure. The JEDI algorithm is summarized in Fig. 1.

## 3 Experimental Results

### 3.1 Simulated Speckle

The first set of experiments utilize simulated speckle to perform controlled evaluations of despeckling performance. The speckle images are simulated according to Eq. 1, where a noise-free reference image  $f(\mathbf{x})$  is multiplied with a unit-mean Rayleigh-distributed random field  $n(\mathbf{x})$ . Correlated noise values are generated by low-pass filtering a complex Gaussian field with a  $3 \times 3$  averaging filter and taking the magnitude [8]. Different noise levels are generated by using various values for the standard deviation of the underlying complex Gaussian field, given by  $\sigma_n$ . The speckle is applied to a synthetic ice floe pattern.

The performance of proposed JEDI algorithm is compared with the Frost filter [3],  $\Gamma$ -MAP [5], GenLik [8], speckle-reducing anisotropic diffusion (SRAD) [6], and the adaptive weighted median filter [7]. Of the popular LLSE methods, we choose the Frost filter as a representative algorithm since it has been shown that the Lee, Frost, and Kuan filters have similar performance [11]. The window size used for all methods is  $3 \times 3$ . In the implementation of

JEDI,  $\alpha = 30$ ,  $\beta = 4$ ,  $\theta = 2$ , and  $h = \text{median}(\sigma(\mathbf{x}))$  are used as those were found to be effective during testing.

To evaluate the performance of the despeckling algorithms we use the PSNR measure as well as the universal image quality index proposed by Wang and Bovik [12]. The index is based on three factors: image correlation, luminance distortion, and contrast distortion. Because JEDI performs contrast manipulation, only the first two factors of the quality index are used for meaningful evaluation. The PSNR and image quality measures are plotted in Fig. 3. In Fig. 2, we show the filtering results for  $\sigma_n = 0.6$ .

The performance measures show that JEDI performs favorably in comparison to the popular despeckling methods, outperforming the other methods in both PSNR and the universal image quality index at all but the highest noise level, where it performed on par with the other methods. On average, JEDI provides a 2-15% improvement in PSNR and a 5-14% improvement in image quality index measures. These quantitative measures agree with the subjective visual results. One can observe that while both the  $\Gamma$ -MAP and median filters do a good job of preserving edge detail, a significant amount of speckle still remains. The Frost and SRAD filtered output suffers noticeable degradation of edge detail. GenLik offers good noise suppression while preserving edges. Finally, the speckle is the least pronounced in the JEDI result, while the edge details are enhanced when compared to the other methods.

### 3.2 SAR Images

The algorithms are applied to portions of two real SAR images collected by RADARSAT-2, using the same parameters as the synthetic image tests. The results are given in Fig. 4 and Fig. 5. For both images, a subjective visual comparison reveals similar characteristics. The  $\Gamma$ -MAP filter, while providing good edge preservation, provides limited noise suppression. The Frost and SRAD methods, while providing good noise suppression, oversmooth the image, resulting in a lack of detail. GenLik is able to provide local detail enhancement as well as good noise suppression. The median filter performs slightly worse than the  $\Gamma$ -MAP filter in terms of noise removal. Finally, JEDI is able to provide the best speckle reduction, while also producing well-defined structure details. JEDI's ability to preserve and enhance structural details can also be seen in Fig. 6, which shows the full image of which Fig. 5 is a portion.

## 4 Conclusion

In this paper, we presented JEDI, a novel method for joint enhancement and despeckling of SAR images using an adaptive stochastic estimation framework. JEDI uses an

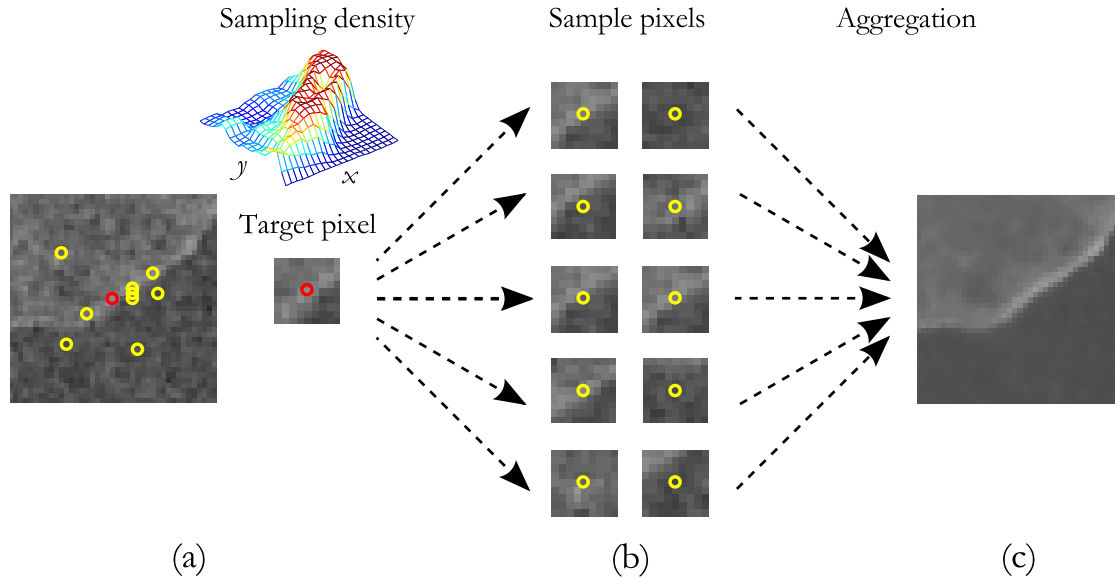


**Figure 1. The JEDI algorithm. (a) The local variance of the target pixel is used to generate a pdf from which (b) sample pixels are drawn. (c) The sample pixels are aggregated using an adaptive weighting scheme with an enhancement term.**

adaptive Monte Carlo sampling approach based on the local statistics to generate a set of pixels that exhibit potential information redundancy. These pixels are then aggregated using an adaptive similarity-based weighting scheme to achieve speckle reduction as well as detail enhancement at the same time. The experimental results demonstrate the effectiveness of the proposed method in achieving high levels of speckle suppression and detail enhancement compared to current popular methods.

## Acknowledgment

This research has been sponsored in part by the Natural Sciences and Engineering Research Council of Canada (NSERC) and GEOmatics for Informed DEcisions (GEOIDE).

## References

- [1] J. W. Goodman, "Statistical Properties of Laser Speckle Patterns," in *Laser Speckle and Related Phenomena.*, J. C. Dainty, Ed. New York: Springer-Verlag, 1984, pp. 9–75.
- [2] J. S. Lee, "Speckle suppression and analysis for synthetic aperture radar," *Opt. Eng.*, vol. 25, no. 5, pp. 636–643, 1986.
- [3] V. S. Frost, J. A. Stiles, K. S. Shanmugan, and J. C. Holtzman, "A model for radar images and its application to adaptive digital filtering for multiplicative noise," *IEEE Trans. Pattern Anal. Machine Intell.*, vol. PAMI-4, pp. 157–165, 1982.
- [4] D. T. Kuan, A. A. Sawchuk, T. C. Strand, and P. Chavel, "Adaptive restoration of images with speckle," *IEEE Trans. Acoust., Speech, Signal Process.*, vol. ASSP-35, pp. 373–383, 1987.
- [5] A. E. Lopes, E. Nezry, R. Touzi, and H. Laur, "Structure Detection and Adaptive Speckle Filtering in SAR Images," *Int. J. Remote Sens.*, vol. 14, no. 9, pp. 1735–1758, 1993.
- [6] Y. Yu and S. T. Acton, "Speckle reducing anisotropic diffusion," *IEEE Trans. Image Process.*, vol. 11, no. 11, pp. 12601270, Nov. 2002.
- [7] T. Loupas, W. McDicken, and P. Allen, "An adaptive weighted median filter for speckle suppression in medical ultrasound images," *IEEE Trans. Circuits Syst.*, vol. 36, pp. 129135, 1989.
- [8] A. Pižurica, W. Philips, I. Lemahieu, and M. Achero, "A Versatile Wavelet Domain Noise Filtration Technique for Medical Imaging," *IEEE Trans. Med. Imag.*, vol. 22, no. 3, pp. 323–331, Mar. 2003.
- [9] Q. Yu and D. A. Clausi, "SAR sea-ice image analysis based on iterative region growing using semantics," *IEEE Trans. Geosci. Remote Sens.*, vol. 45, no. 12, part 1, pp. 3919–3931, Dec. 2007.

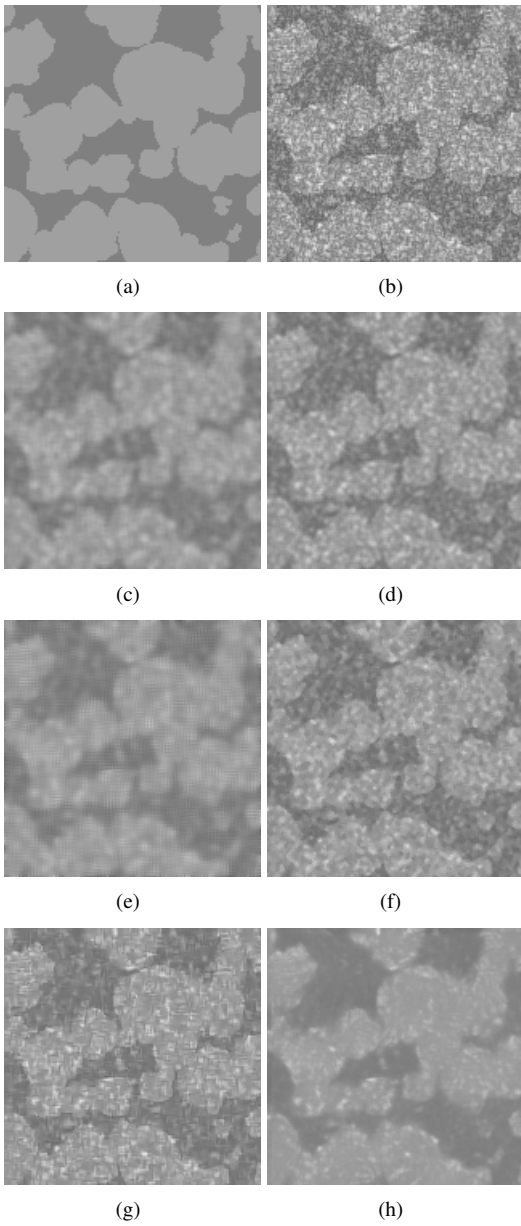


**Figure 2. Despeckling of the synthetic ice image. (a) Noise-free reference image. (b) Simulated speckle with  $\sigma_n = 0.6$ . The noisy image is processed using (c) Frost filter, (d)  $\Gamma$ -MAP (e) SRAD, (f) median filter, (g) GenLik, (h) and JEDI.**

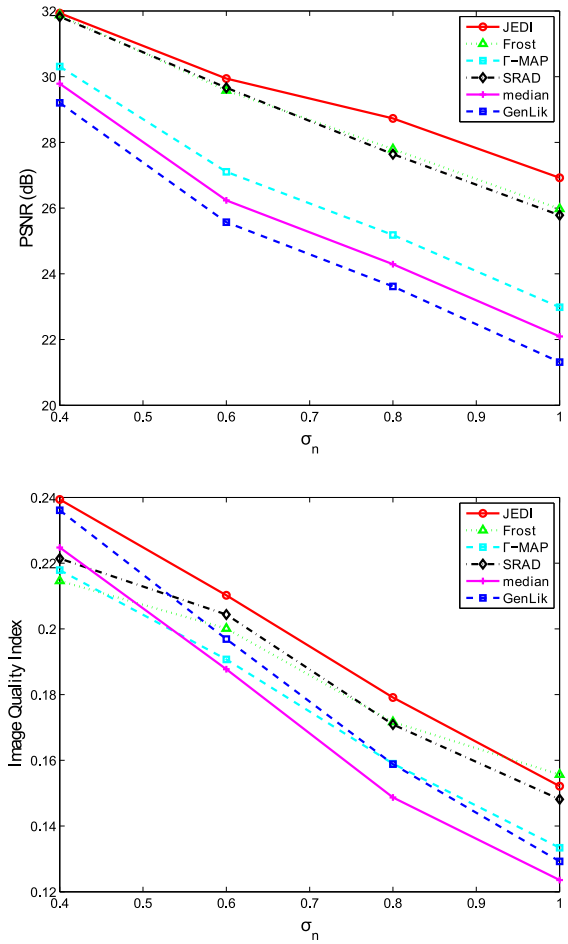


**Figure 3. PSNR and Image Quality Index performance measures for the synthetic ice image for varying noise levels.**

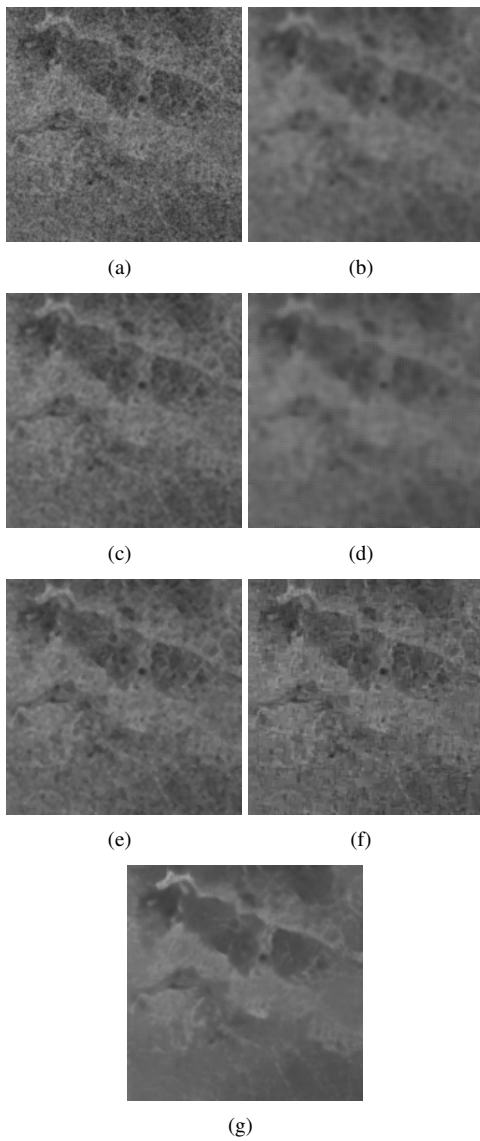


**Figure 4. (a) First RADARSAT-2 test image. The image is processed with (b) Frost filter, (c)  $\Gamma$ -MAP, (d) SRAD, (e) median filter, (f) Gen-Lik, and (g) JEDI.**

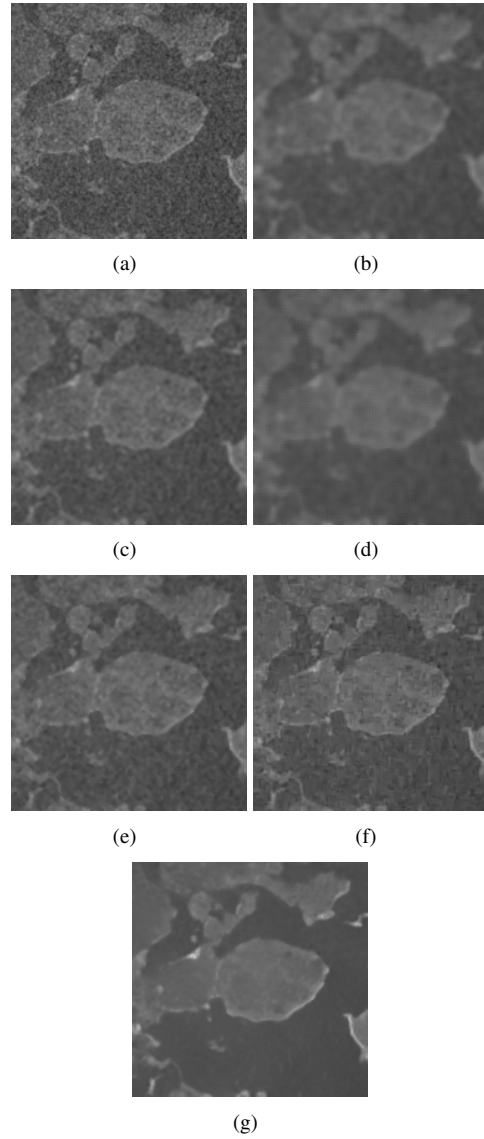
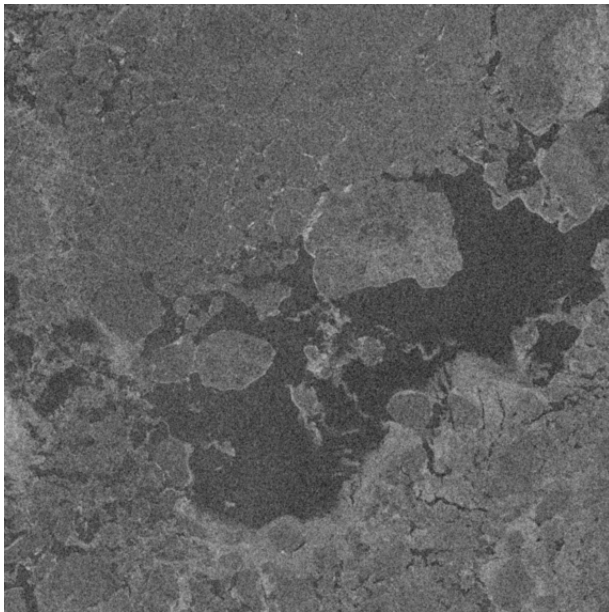
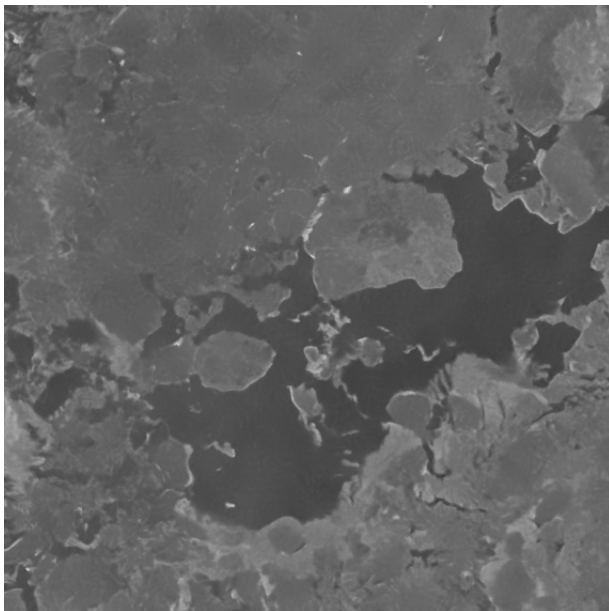


**Figure 5. (a) Second RADARSAT-2 test image. The image is processed with (b) Frost filter, (c)  $\Gamma$ -MAP, (d) SRAD, (e) median filter, (f) Gen-Lik, and (g) JEDI.**



(a)



(b)

**Figure 6. (a) The full SAR image from Fig. 5 and (b) the image processed with JEDI, where it is able to preserve much of the structural details.**

- [10] A. Wong, A. Mishra, P. Fieguth, and D. A. Clausi, "An Adaptive Monte Carlo Approach to Nonlinear Image Denoising," in *Proc. Int. Conf. Pattern Recognition (ICPR)*, 2008.
- [11] J. M. Park, W. J. Song, and W. A. Pearlman, "Speckle filtering of SAR images based on adaptive windowing," in *Proc. Inst. Elect. Eng. Vis. Image Signal Process.*, vol. 146, no. 4, 1999.
- [12] Z. Wang and A. Bovik, "A universal image quality index," *IEEE Signal Process. Lett.*, vol. 9, no. 3, pp. 8184, Mar. 2002.